Statistical analysis of particulate interface lengths in diffusion bonded joints in a metal–matrix composite

P. G. PARTRIDGE, M. SHEPHERD*, D. V. DUNFORD
Materials and Structures department, Royal Aerospace Establishment, Farnborough, Hampshire, UK

A statistical analysis has been made of the number and length of particle–particle (P–P), particle–matrix (P–M) and matrix–matrix (M–M) interfaces present in solid state and liquid phase diffusion bonded joints in a particulate metal matrix composite (17 vol % SiC/Al–Li 8090 alloy). All solid state bonds had planar bond interfaces with the polished particle facets aligned in and parallel to the bond interface. The particle interface lengths in 400 μm long sample lengths in the L direction in a bond interface could vary from zero to over 50% of the sample length, with typical values for a random sample of 8% and 22% for P–P and P–M interfaces, respectively.

Liquid phase diffusion bonded joints contained a higher volume fraction of particles in the bond region, but the bond interface was non-planar and particle interfaces were not aligned.

The significance of these results for the strength and processing of diffusion bonded composites is discussed.

1. Introduction

It is difficult to diffusion bond (DB) aluminium alloys because of the stable surface oxide film [1]. Interlayer coatings or foils of Cu, Ag or Zn have been used to facilitate bonding of these alloys, but the composition in the bond interface region is changed and the bond strength is sensitive to residual intermetallic phases at the bond line [2–6]. In Li containing aluminium alloys the surface oxide film is less protective [7, 8] and solid state diffusion bonded joints have been made between 8090 Al–Li alloy sheets without interlayers [4, 5, 9]. The shear strengths of these joints were similar to that of the base metal.

Diffusion bonding is a particularly attractive method for joining metal–matrix composites (MMCs) since it avoids the degradation associated with fusion welding or the practical problems encountered in friction welding. Some preliminary experiments [5] have shown that solid state and liquid phase diffusion bonds (LPDB) can be made between a composite containing 17% by volume of SiC particles in 8090 alloy. The significant area fraction of particle interface present in the composite surface suggests however, that the strength of a diffusion bonded joint will be dependent on the type, size, number and distribution of particle interfaces at the bond line.

In order to select the bonding process parameters for optimum strength and toughness it is necessary to characterize the microstructure at the bond interface. As part of this characterization a statistical analysis of each type of interface present and of the variability of the microstructure in the bond line has been carried out. The results of this analysis are described in this paper.

2. Experimental procedure

The 8090 alloy composition (wt%) was Al–2.4Li–1.2Cu–0.6Mg. The metal matrix composite was made by BP Research International and rolled to sheet at RAE. The sheet surfaces were mechanically polished to 1 μm diamond surface finish prior to diffusion bonding by vacuum hot pressing as described elsewhere [4, 9]. A schematic diagram of a section normal to the sheet surface is shown in Fig. 1. If an infinitely thin cut is made in the MMC parallel to the sheet surface, the particles would be cut along A–A in Fig. 1a and if the cut surfaces are bonded without displacement the interfaces created at the bond line would be as shown. Displacement in the bond plane would create new interfaces as shown in Fig. 1b; these are characteristic of DB joints.

The bond interface microstructure in a solid state DB joint in a section (L–ST plane) normal to the bond plane and parallel to the rolling direction is shown in Fig. 2a and b. The bond line A–A can be identified by the flat facets on the SiC particles lying in the bond line at B in Fig. 2a and b. The particle facet in one polished sheet surface may coincide with a similar particle facet in the opposite sheet surface to produce

* Vacation student, University of Surrey.

0022–2461/91 $03.00 + .12

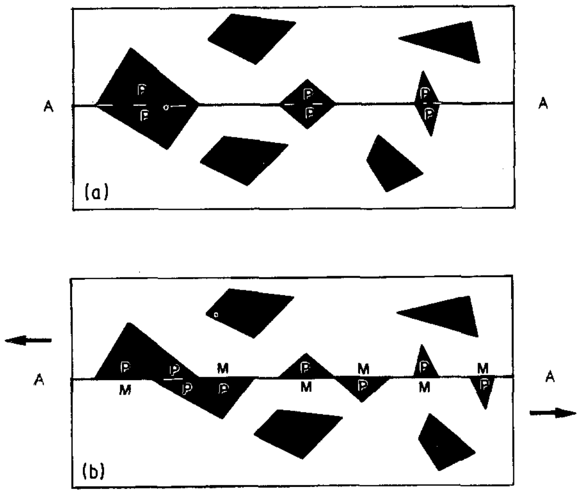

Figure 1 Schematic diagram of bond interface A–A produced by cutting and rebonding (a) without displacement. (b) after small relative displacement along A–A to produce a symmetrical bond interface. (P particle, M matrix)

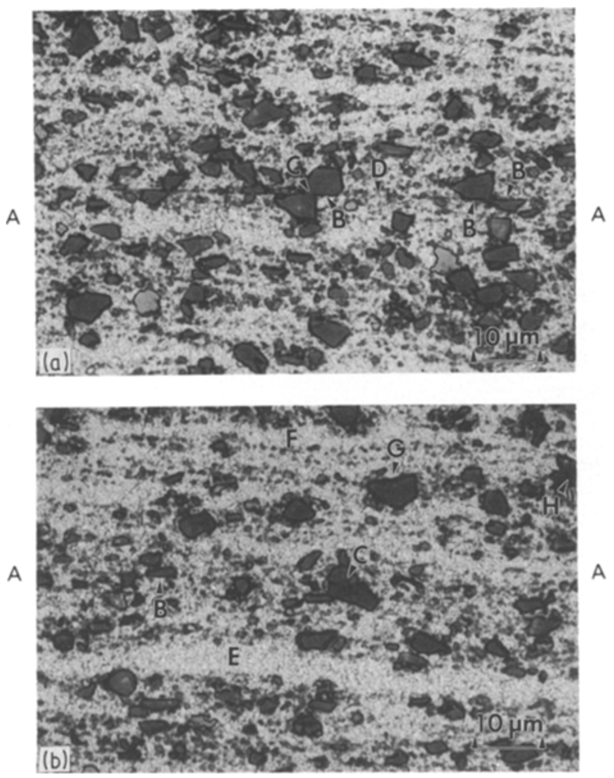

Figure 2 Optical micrographs of random samples in bond interface at A–A in MMC. B = P–M interface, C = P–P interface, D = M–M interface, in bulk material banding at E, F and short P–P interface and long straight P–M interface at H and G, respectively.

a particle–particle (P–P) interface (Fig. 1 and C in Fig. 2a and b) or the facet may form an interface (P–M) with the matrix (Fig. 1 and B in Fig. 2a and b). As expected in the bond line matrix–matrix (M–M) interfaces (Fig. 1 and D in Fig. 2a and b) were usually the most extensive whereas in the base metal P–M interfaces dominated.

In carrying out the statistical analysis it was difficult to obtain a satisfactory sample size. To make the interface length measurements a high magnification print was required, which in practice limited the maximum individual sample lengths over which measurements could be made to 100 µm. This sample length did not provide a statistically significant number density. Since the measurements were time consuming a compromise was necessary and it was decided to measure four separate 100 µm lengths. The statistical data are presented for each sample length $L = 100$ µm only for the random sample in the bond line in order to show the variability between these sample lengths; all other data are based upon four 100 µm lengths taken together i.e the sample length $L = 4 \times 100 = 400$ µm.

The statistical data were obtained from polished and slightly etched sections. The original micrograph was obtained at $\times 1000$ magnification and measurements were made on photographic prints at $\times 2200$ magnification. The length and number of interfaces of the type P–P, P–M and M–M were measured over a sample length $L = 100$ µm on each print in the longitudinal direction and along the bond line or in the bulk material or in the LPDB joint, as described in Table I. The parameters defined in Table II [10] were

TABLE I Origin and dimensions of sample used for analysing interfaces

Origin of sample	Sample size and position
Solid state db joint (bond line)	Four random lengths, $L = 100$ µm
	Four selected lengths, $L = 100$ µm in regions of minimum particle density
Liquid phase db joint (bond line)	Four random lengths, $L = 100$ µm in centre of high particle density region
In bulk material (parallel to sheet surface)	Four selected lengths, $L = 100$ µm in regions of maximum particle density

TABLE II Parameters and nomenclature used in statistical analysis

x = interface (intercept) length
n = number of interfaces
Σx = total length of interfaces
$\bar{x} = \frac{\Sigma x}{n}$ = arithmetic mean length of interfaces
$s = \left(\frac{\Sigma(x-\bar{x})^2}{n}\right)^{1/2}$ = standard deviation of interface lengths from mean
Mode = most frequently occurring interface length
Median = middle interface length after the lengths have been arranged in ascending order
95% confidence limits = 95% of the interface lengths lie within these limits
$S = \frac{\bar{x} - \text{mode}}{s}$ = Pearson's coefficient of skewness
L = total sample length
Ratio
$R = \frac{\Sigma x}{L} \times 100$ = percentage interface length over total sample length
P–P = particle–particle interface
P–M = particle–metal interface
M–M = metal–metal interface
P = particle intercept

obtained for each type of interface i.e. interface length x, mean $\bar{x}$ and standard deviation s, mode, median, 95% confidence limits, coefficient of skew S, total interface length and the ratio R, the total interface length expressed as a percentage of the total sample length L. A schematic illustration of mode, median and x is given in Fig. 3. Note that all the data are based upon line intercept lengths measured in the rolling direction only and in the L–ST plane. The two- or three-dimensional interface distribution was not quantified. Some alignment of particles in the rolling direction was apparent which implies different interface distributions could be obtained in other directions.

3. Results

3.1. Microstructure of diffusion-bonded joints

In the MMC the SiC particle distribution was very uniform on a macroscopic scale but on a microscopic scale some banding (at E and F in Fig. 2b) and clustering (at A in Fig. 4) of the particles was apparent, leading either to bands completely free of particles (at E in Fig. 2b) or to bands containing a higher than average density of particles (Fig. 4) over the individual sample lengths of 100 μm. No regions completely free of particles or regions containing a higher than average density of particles were, however, actually detected on the bond line in the present samples.

Random samples in the solid state bond line are shown in Fig. 2a and b; the three types of interface (P–P, P–M, M–M) are indicated along the bond line A–A. Note the marked planarity of the bond interface. Some short P–P and long straight P–M interfaces were also present in the bulk material (at H in Fig. 2a and G in Fig. 2b, respectively), but the solid state bonded joint was unique in having these interfaces in and oriented parallel to the bond interface plane.

Selected minimum particle density samples in the solid state bond line were found to lie in regions where banding was more apparent. In order to obtain an indication of the maximum possible particle *interface* density in a bonded joint in this MMC, values for the particle (P) line *intercept* number n and length x were obtained in regions of maximum particle density in the bulk material (Fig. 4 and Table I). The intercept line is shown schematically in Fig. 1a. Using these values and assuming a bond is made by cutting along this intercept line, it is possible to predict the corresponding particle *interface* (P–P and P–M) values for bonds made as follows:

1. Surfaces cut and rebonded.

(a) With complete particle coincidence, as in Fig. 1a the P intercepts (number n and length x) become P–P interfaces of number n and length x.

(b) With displacement (Fig. 1b) and no particles coincident, the P intercepts become P–M interfaces of number $2n$ and length x.

2. One cut surface bonded to another surface with zero particle density. The P intercepts become P–M interfaces of number n and length x.

Predictions in 1a and b represent the maximum values for these extreme examples; in practice the values will fall between these extremes.

A random sample in the liquid phase diffusion bonded joint is shown in Fig. 5. This joint could be distinguished from the solid state bonded joint by

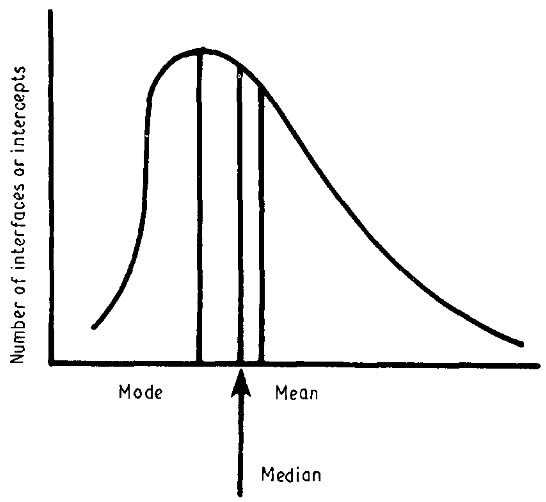

Figure 3 Schematic diagram illustrating mode, mean and median interface length or particle intercept length defined in Table II.

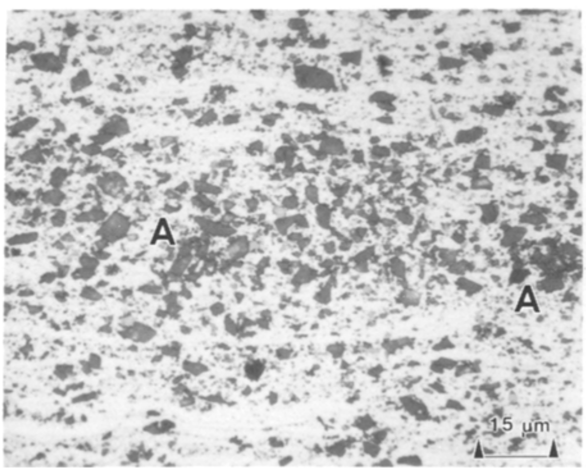

Figure 4 Optical micrograph of selected sample in region of high particle density in bulk MMC. Particle clustering at A.

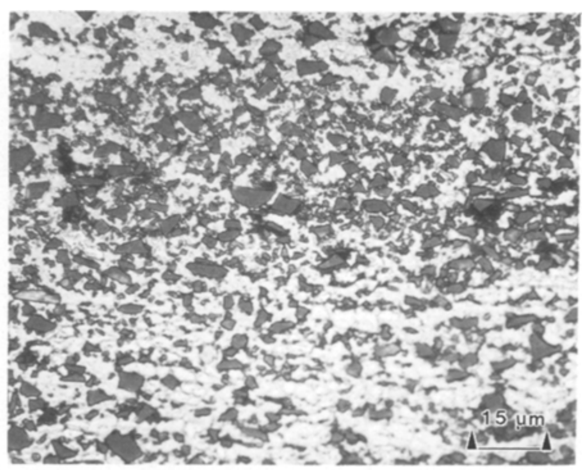

Figure 5 Optical micrograph of random sample of band of high particle density in LPDB joint.

1. a band in the bond region containing a higher volume fraction of particles;

2. the uniformity of the high particle density band in three dimensions parallel to the bond plane;

3. the absence of a planar interface and of preferred orientation of the polished particle interfaces along the bond line.

Otherwise the microstructure in this bond region was very similar to that in the bulk material i.e. the particles were mostly uniformly spaced and surrounded by the matrix. Particle intercept measurements were made at the centre of the band of high particle density and were compared with data for the maximum particle density in Fig. 4.

3.2. Statistical data for random sample lengths of 100 and 400 μm in the bond line

Data obtained for four 100 μm sample lengths are summarized in Table III. The number of P–P interfaces per 100 μm length was in the range $n = 3$ to 9 compared with $n = 13$ to 21 for P–M interfaces. The mean length was for P–P interfaces $x = 1.23$ to 1.4 μm and for P–M interfaces $x = 1.23$ to 1.59 μm. The fraction of the bond line $L = 100$ μm occupied by these interfaces was $R = 3.7$ to 12.6% for P–P and $R = 13.5$ to 27% for P–M. These data are plotted in Fig. 6 together with the 95% confidence limits. The variability in the data for these four sample lengths is apparent in the values for the standard deviation s, the 95% confidence limits and the coefficient of skewness S in Table III.

The data for the $L = 100$ μm lengths were taken together to give the values in Table IV for a random 400 μm sample length in the bond line. The interface length distribution is plotted in Fig. 7 and shows positive skew. These data show $R = 8\%$ for P–P and 22% for P–M interfaces. Thus the total interface length occupied by P/P + P/M interfaces was $R \sim 30\%$ with maximum interface lengths of ~ 4 μm for P–P and 6 μm for P–M (Fig. 7).

3.3. Statistical data for a selected sample length of 400 μm in regions of minimum particle density in the bond line

The corresponding data for the four 100 μm sample lengths are reported elsewhere [11]. Data taken over the 400 μm sample length are summarized in Table IV and Fig. 8. The ratio $R = 2.8\%$ for P–P interfaces and 18.3% for P–M interfaces to give a total P/P + P/M of 20%. The maximum interface lengths x_{max} were 3 μm for P–P and 5 μm for P–M. Compared with the random sample, in the low particle density region the R value was about 1/3 for the P–P interface and similar for the P–M interface.

3.4. Statistical data for a selected sample length of 400 μm in regions of high particle density in the bulk material

To predict the interfaces that might arise if a bond plane intercepted a region of high particle density, particle intercept lengths were measured along four selected lengths of 100 μm in regions of high particle density in the bulk material as shown in Fig. 1a. Data for the four 100 μm sample lengths are reported elsewhere [11]. Data for the 400 μm sample length are summarized in Table IV and plotted in Fig. 9. Note the large number ($n = 79$) of particle intercepts which totalled $R = 49.5\%$ of the sample length (Table IV). Assuming a cut and re-bond as in Fig. 1b, the P/P + P/M interface lengths could greatly exceed 50% of the sample length with a maximum individual P–M *interface* length up to 2 × maximum P *intercept* length i.e. 19 μm (Fig. 9).

3.5. Statistical data for a random sample length of 400 μm in the liquid phase diffusion bond

The data obtained for the four 100 μm sample lengths were taken together and are summarized in Table IV and plotted in Fig. 10. The number of intercepts was

TABLE III Intercept lengths for particle–particle, particle–metal and metal–metal determined for four random lengths L in bond interface[a]

Sample lengths L	Type of interface	Statistical parameters n	Σx (μm)	$\bar{x}$ (μm)	s (μm)	Mode (μm)	Median (μm)	95% confidence limit (μm)	S	R (%)
1	P–P	7	9.45	1.35	1.07	1.35	1.35	0.45–3.6	0	9.5
	P–M	21	26.55	1.26	1.07	0.45	0.9	0.45–3.15	+ 0.76	26.6
	M–M	19	59.4	3.13	2.47	2.25	2.25	0.45–6.75	+ 0.36	59.4
2	P–P	9	12.6	1.4	0.97	1.13	1.35	0.45–3.6	+ 0.28	12.6
	P–M	11	13.5	1.23	1.03	0.9	0.9	0.45–4.05	+ 0.32	13.5
	M–M	22	70.2	3.19	3.59	0.9	1.35	0.45–10.35	+ 0.64	70.2
3	P–P	3	3.68	1.23	0.96	—	0.92	0.46–2.3	—	3.7
	P–M	13	20.7	1.59	1.56	0.46	0.92	0.46–5.52	+ 0.72	20.7
	M–M	16	70.84	4.43	4.42	0.46	3.22	0.46–15.64	+ 0.9	70.8
4	P–P	5	6.75	1.35	1.00	0.9	0.9	0.9–3.15	+ 0.45	6.8
	P–M	19	27	1.42	1.13	0.45	0.9	0.45–4.05	+ 0.86	27
	M–M	17	64.35	3.79	2.71	1.8	2.7	0.45–10.35	+ 0.73	64.4

[a] Four lengths $L = 100$ μm each measured in bond interface in L–ST plane.

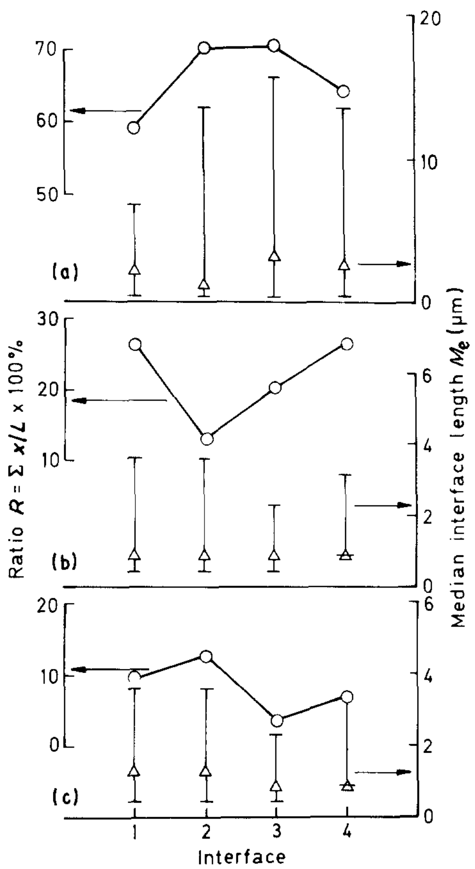

Figure 6 Interface lengths for (a) M–M, (b) P–M and (c) (P–P) interfaces determined for four random sample lengths of $L = 100$ μm in the MMC–MMC diffusion bond interface (bars indicate 95% confidence limits).

$n = 84$ for particles P and $n = 10$ for P–M interfaces; these values were slightly greater than those for the high particle density region but the mean particle size x was much smaller and consequently for the particle intercept $R = 34\%$ for the LPDB, which was much smaller than for the high particle density region. Thus although the volume fraction of particles in the bond region was greater than for the surrounding regions in the base metal, the total R value (P + P–M) for LPDB was close to that for the (P–P + P–M) value obtained for random samples in the solid state MMC–MMC bond (Table IV). For LPDB the maximum intercept lengths were 7 μm for P and 1 μm for P–M.

4. Discussion

In spite of the difficulty in sampling the composite microstructure the results of the analysis allow tentative comparisons to be made of the size and distribution of particle interfaces in bonded joints made by the two methods. The bond strength will be dependent primarily on the four parameters listed in Table V, namely the number density n, the mean $\bar{x}$ and maximum x_{max} particle interface length, and the fraction of the bond line occupied by the particle interfaces R. For the samples taken in the bond line the mean particle interface lengths for P–P and P–M interfaces were similar at $x = 1.35$ to 1.38 μm for random samples and for selected samples in regions of minimum particle density; the maximum interface lengths were also similar ($x = 3$ to 4 μm for P–P and $x = 5$ to 6 μm for P–M). The percentage length occupied by the interfaces, R, was greater in the random sample particularly for the P–P interfaces ($R = 8\%$ for P–P and $R = 22\%$ for P–M) than in the region of minimum particle density ($R = 2.8\%$ for P–P and $R = 18.3\%$ for P–M).

Relative to the above random samples, in the high particle density regions of the bulk material and in the liquid phase diffusion bonded region particle *intercept* numbers n were much larger at $n \sim 80$ (Table V), with a particularly large maximum P–M *interface* length of $2 \times P_{max} = 19$ μm predicted for the high particle density region (see Section 3.1). The total R values for the random (P/P + P/M interfaces) and LPDB (P + P/M) samples were, however, close (30% and 34%, respectively) and much less than the value of 50.4% for (P + P/M) in the maximum particle density sample in the bulk material (Table V). The surprisingly

TABLE IV Intercept lengths for particles (P) and interface lengths for particle–particle (P–P), particle–metal (P–M) and metal–metal (M–M) determined for a sample length $L = 400$ μm in L–ST plane

		Statistical parameters								
	Type of intercept	n	Σx (μm)	$\bar{x}$ (μm)	s (μm)	Mode (μm)	Median (μm)	95% confidence limit (μm)	S	R (%)
In bond interface										
	P–P	24	32.48	1.35	0.92	0.90	0.91	0.45 to 3.6	+ 0.49	8.1
Random lengths	P–M	64	87.75	1.37	1.20	0.45	0.9	0.45 to 4.14	+ 0.77	21.9
	M–M	74	264.79	3.58	3.40	0.45	2.25	0.45 to 11.25	+ 0.92	66.2
Selected lengths in low particle density regions	P–P	8	11.02	1.38	0.86	0.46	1.37	0.46 to 2.76	+ 1.07	2.8
	P–M	53	73.29	1.38	1.12	0.46	0.92	0.45 to 4.14	+ 0.82	18.3
	M–M	65	312.29	4.80	6.52	2.30	2.76	0.9 to 15.18	+ 0.38	78.1
Selected intercept lengths in high particle density regions in parent metal	P	79	197.91	2.51	1.71	1.35	1.84	0.45 to 5.52	+ 0.68	49.5
	P–M	3	3.61	1.20	0.76	—	0.9	0.46 to 2.25	—	0.9
	M	77	192.83	2.50	2.02	0.5	1.84	0.45 to 6.44	+ 0.99	48.2
Random intercept lengths in liquid phase diffusion bond	P	84	135.36	1.61	1.31	0.94	0.94	0.47 to 5.17	+ 0.51	34
	P–M	10	5.64	0.56	0.20	0.47	0.47	0.47 to 0.94	+ 0.45	1.4
	M	98	238.76	2.44	2.16	0.94	1.41	0.47 to 8.93	0.69	60

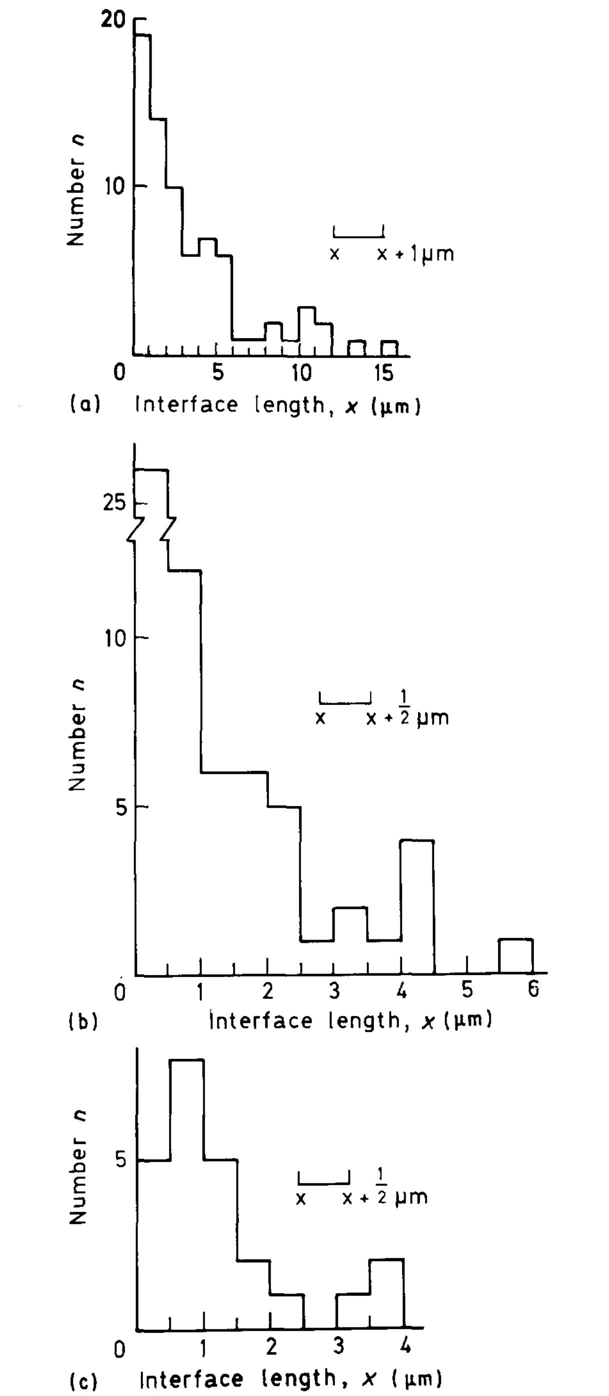

Figure 7 Distribution of the interface lengths for (a) M–M, (b) P–M and (c) P–P interfaces averaged over $L = 4 \times 100$ μm random sample lengths in the MMC–MMC diffusion bond interface.

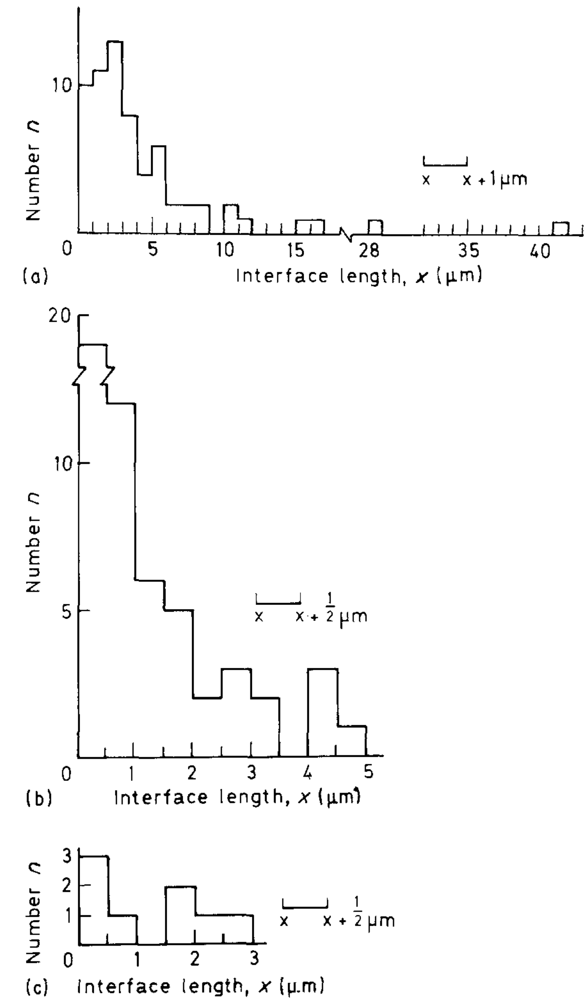

Figure 8 Distribution of the interface lengths for (a) M–M, (b) P–M and (c) P–P interfaces averaged over $L = 4 \times 100$ μm selected sample lengths in regions of minimum particle density in the MMC–MMC diffusion bond interface.

low R value for the LPDB could be a consequence of the advance of a planar melt front during bonding [12]. These results show clearly that a wide range of R values are possible depending on the position of the bond plane.

The three interfaces considered in the present analysis (P–P, P–M and M–M) could each make a different contribution to the strength and ductility of the bonded joint. For significant particle interface area fractions in the bond plane the bond ductility would be expected to be in the order M–M $\gg$ P–M $>$ P–P. Assuming the P–P and possibly P–M interfaces had little strength after bonding, then values of x and n obtained for these interfaces could be an indication of the number and length of cracks present in the bond interface after bonding.

Preliminary shear strength data for solid strength diffusion bonded joints in the 8090 matrix alloy and in the MMC–MMC joint have been reported as 190 and 100 MPa, respectively [11]. This represents a reduction in the bond strength in the MMC of 47% relative to the matrix bond strength. Assuming the P–P and P–M interface strengths are negligible, then the predicted strength reduction in the MMC–MMC joint is between 30% (based on the random sample data, Table V) and $>$50% (based on the high particle density sample, Table V). This suggests that the regions of high particle density may contribute significantly to the reduction in strength.

Solid state bonding has the disadvantage that it normally leads to a planar bond interface both in the Al–Li alloy [4, 9] and in the Al–Li alloy MMC [4] and in the latter the particulate interfaces were aligned in this bond interface. This would favour more rapid crack growth in the bond plane under static or dynamic loading.

In the LPDB the bonding pressure was much lower than for solid state bonding and there was no planar bond interface and no alignment of the P–P or P–M

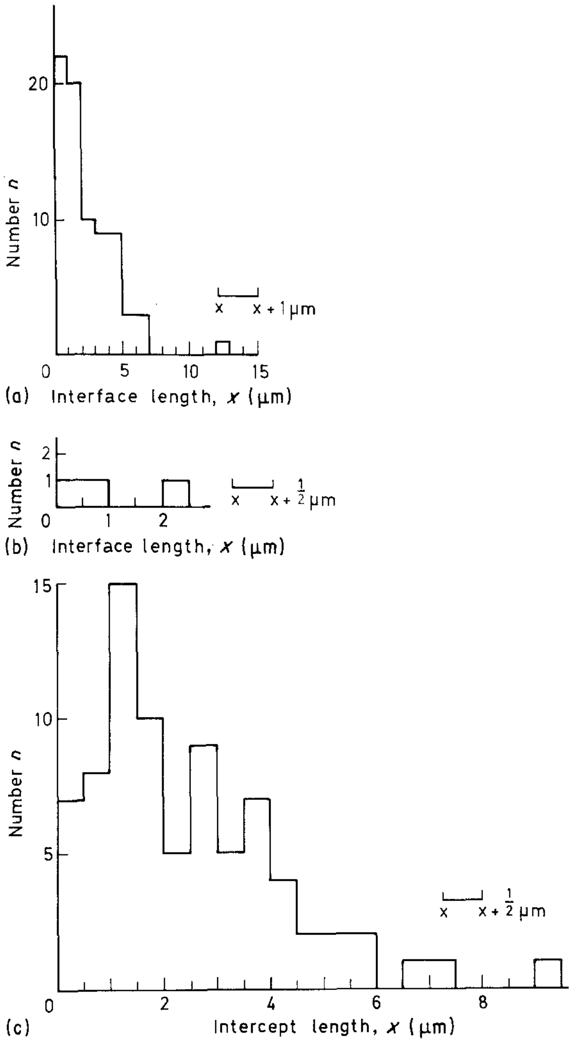

Figure 9 Distribution of the particle intercept P and P–M and M–M interface lengths averaged over $L = 4 \times 100$ μm selected sample lengths in regions of high particle density in the bulk MMC.

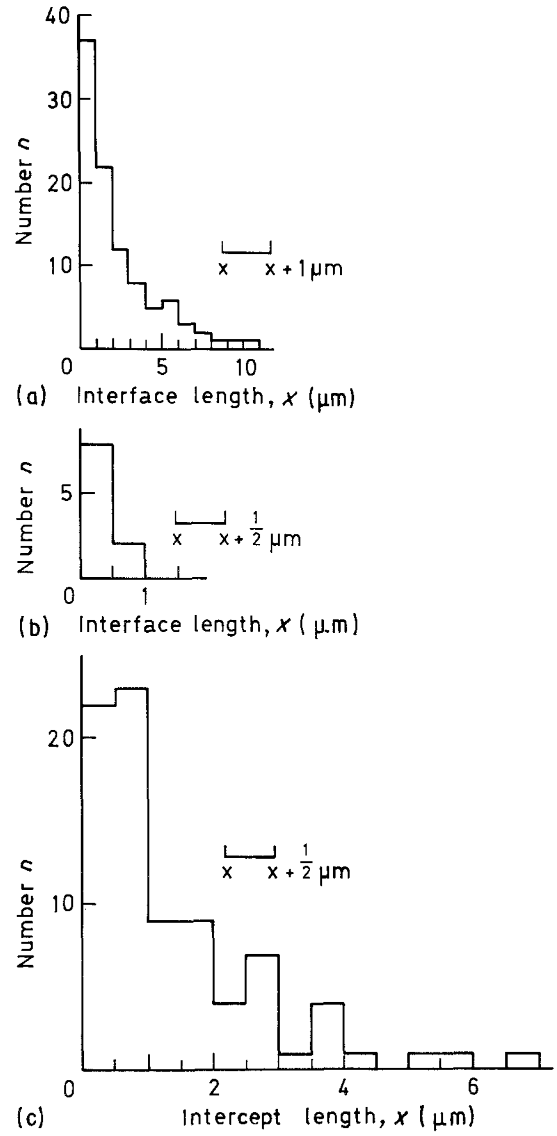

Figure 10 Distribution of the particle intercept P and P–M and M–M interface lengths averaged over $L = 4 \times 100$ μm random sample lengths in the liquid phase diffusion bonded interface.

interfaces. The particles present were distributed uniformly in three dimensions throughout the bond region, and although the higher volume fraction would tend to reduce the local ductility, the uniform particle spacing could lead to higher bond strength. This is consistent with measured bond strengths for LPDB joints, which were greater than for MMC–MMC but less than for the matrix–matrix bonded joint.

The MMC–MMC bond interface may be symmetrical or asymmetrical with respect to the particle distribution on either side of the bond plane depending upon where the bond plane occurs in the base metal e.g. it may intersect regions containing 0 vol % or greater than 50 vol % particles (Table V). This may contribute to the scatter in bond strength and ductility. The local fracture behaviour may also reflect this microstructural variability and this should be distinguished from surface finish or contamination effects in fractographic studies of diffusion bonded joints. The SiC particle size range and particle distribution may be especially important for applications such as metallic laser mirrors or high speed rotating mirrors [13]. Further work is therefore required to relate the particulate interface parameters determined in this paper to the physical and mechanical properties of metal matrix composites.

5. Conclusions

The conclusions are as follows.

1. In the MMC–MMC solid state diffusion-bonded joint the interface was planar and the particle interfaces were aligned parallel in this interface. The liquid phase diffusion-bonded joint had a non-planar interface, a uniformly higher particle density in the bond region and the particle interfaces were not aligned.
2. Statistical analysis of the particle–particle (P–P) and particle–matrix (P–M) interfaces in a bonded joint in the L direction in the L–ST plane in 17 vol % SiC–Al-Li 8090 alloy has indicated considerable variation in the microstructure is possible at the bond line.
3. The percentage of the bond line occupied by the particle *interfaces* R was 8% and 22% for P–P and P–M, respectively in a random sample. For particle *intercept* lengths, $R = 35\%$ in a liquid phase diffusion-bonded joint compared with $R = 50\%$ for regions of high particle density in the bulk material.
4. The relative strengths of the bonded joints were predicted to be matrix–matrix > MMC–LPDB–

TABLE V Summary of important particle intercept and particle interface parameters for different samples

Position of sample	Intercept type	n	$\bar{x}$ (μm)	R (%)	x_{max} (μm)
Bond line	P–P Interface	24	1.35	8.1	4
Random	P–M Interface	64	1.37	21.9	6
Minimum particle density region	P–P Interface	8	1.38	2.8	3
	P–M Interface	53	1.38	18.3	5
Liquid phase diffusion bonded joint	P Intercept	84	1.61	34	7
	P–M Interface	10	0.56	1.4	1
Bulk Material					
Minimum particle density region	P Intercept	0	—	0	—
	P–M Interface	0	—	0	—
Maximum particle density region	P Intercept	79	2.51	49.5	9.5
	P–M Interface	3	1.20	0.9	2.5

MMC > MMC–MMC. This agrees with preliminary shear strength data.

5. The present data suggest that the high R-values for the high particle density regions could contribute significantly to the reduction in MMC–MMC bond strength relative to the matrix–matrix bond strength.

References

1. P. G. PARTRIDGE, NATO-AGARD Lecture series on Superplasticity, No. 168, Sept (AGARD, 1989) Chap. 5.
2. J. HARVEY, P. G. PARTRIDGE and A. LURSHAY, *Mater. Sci. Engng J.* **79** (1986) 191.
3. M. R. EDWARDS, E. KLINKLIN and V. E. STONEHAM, 5th Al–Li Conference, Williamsburg, edited by T. H. Sanders, E. A. Starke, P.-J. Winkler, H. Stoklossa and R. Grimes (1989) p. 431.
4. P. G. PARTRIDGE and D. V. DUNFORD, Superplasticity in Metals, Ceramics and Intermetallics, Materials Research Society, edited by M. J. Mayo, M. Kabayashi and J. Wadsnorth, Vol. 196 (1990) p. 143.
5. D. W. LIVESEY and N. RIDLEY, Diffusion Bonding, Proceedings International Conference, Cranfield. March (Elsevier, 1991) p. 83.
6. R. A. RICKS, T. H. SANDERS, E. A. STARKE, P.-J. WINKLER, H. STOKLOSSA and R. GRIMES (eds) 5th International Al–Li Conference, Williamsburg (1989) p. 441.
7. P. G. PARTRIDGE and N. C. CHADBOURNE, *J. Mater. Sci.* **24** (1989) 2765.
8. P. G. PARTRIDGE, *Int. Mater. Rev.* **35** (1990) 37.
9. D. V. DUNFORD and P. G. PARTRIDGE, *J. Mater. Sci.* **25** (1990) 4957.
10. J. D. LEE and T. D. LEE, "Statistics and Computer Methods in Basic" (Van Nostrand, Amsterdam, 1982).
11. P. G. PARTRIDGE, M. SHEPHERD and D. V. DUNFORD, RAE Tech Report 90024 (1990).
12. I. TUAH-POKU, M. DOLLAR and T. B. MASSALSKI, *Met. Trans.* **19A** (1988) 675.
13. M. HUNT, *Mater. Engng* **8** (1990) 33.

Received 15 June
and accepted 3 July 1990